Crustal-scale convection and diapiric upwelling of a partially molten orogenic root (Naxos dome, Greece)

Olivier Vanderhaeghe, Seth C. Kruckenberg, Muriel Gerbault, Laure Martin, Stéphanie Duchêne, Etienne Deloule

Crustal-scale convection and diapiric upwelling of a partially molten orogenic root (Naxos dome, Greece)

O. Vanderhaeghe[a,*], S.C. Kruckenberg[b], M. Gerbault[a], L. Martin[c], S. Duchêne[a], E. Deloule[d]

[a] GET, Université de Toulouse, CNRS, IRD, UPS, (Toulouse), France
[b] Boston College, Dept Earth & Environmental Sciences, 140 Commonwealth Avenue, Chestnut Hill, MA 02467, USA
[c] School of Earth and Environment, The University of Western Australia, Perth, Australia
[d] CRPG-CNRS, 15 rue Notre Dame des Pauvres, 54501 Vandoeuvre les Nancy, France

ARTICLE INFO

Keywords:
Naxos dome
Cyclades
Geology
Migmatites
U-Pb geochronology
Zircon
Monazite
Crustal-scale convection
Diapirism

ABSTRACT

The goal of this paper is to use the structural, metamorphic and geochronological record from the migmatitic core of the Naxos dome (Greece) and its associated subdomes to address the internal dynamics of a partially molten orogenic root. U-Pb ages from ca. 24 to 16 *Ma* and textures of zircon in the migmatites suggest successive dissolution and precipitation cycles with a period of 1 to 2 *Ma*, interpreted as the timescale of convective instabilities in a ca. 20 km thick partially molten layer. Dimensional analysis indicates that convection of this root requires a viscosity lower than 10^{18} Pa·s, consistent with viscosity values expected for partially molten felsic rocks. Structural analysis and U-Pb geochronology of deformed granitic dikes rooting in the migmatites record the subsequent development of the Naxos dome by diapirism from ca. 16 to 13 *Ma*. The size of the first order migmatite dome on Naxos (5 × 12 km) requires that the unstable layer at the onset of diapirism was 5 to 10 km thick and presented a moderate viscosity contrast with its envelope. From this analysis we propose that the Naxos migmatite dome documents a two stage dynamic evolution for the partially molten root of the Aegean belt characterized by (1) crustal scale convection for at least 8 *Ma* and (2) diapirism for about 3 *Ma* during progressive thinning of the collapsing orogenic crust.

1. Introduction

Gneiss domes are ubiquitous features of the deep crust (Eskola, 1948; Whitney et al., 2004; Yin, 2004). They have been variously interpreted as reflecting (i) interference patterns related to polyphase folding (Myers and Watkins, 1985; Ramsay, 1967; Steck et al., 1998), (ii) flow of a low viscosity layer into dilation sites created by heterogeneous deformation (Brun et al., 1981; Davis and Lister, 1988; Rey et al., 2011), and (iii) buoyant flow of low density and low viscosity partially molten rocks (Brun et al., 1981; Ramberg, 1980; Schwerdtner, 1982). These different models are not mutually exclusive and a variety of processes might be at play during the development of gneiss domes (Burg et al., 2004; Kruckenberg et al., 2011; Vanderhaeghe, 2009). Some of these domes are cored by diatexite migmatite (i.e. former magmas) and mantled by metatexite migmatite (i.e. former partially molten rocks) generated as a consequence of thermal relaxation following the thickening of orogenic crust (Thompson and Connolly, 1995; Vanderhaeghe et al., 2003; Vanderhaeghe, 2012). A key feature of many migmatite domes is the presence of second order domes designated as subdomes (Ledru et al., 2001; Kruckenberg et al., 2011; Vanderhaeghe, 2004; Whitney et al., 2004). We argue here that the Naxos dome (Cyclades, Greece) and its associated subdomes witness gravitational instabilities within a partially molten orogenic crust, in agreement with pioneering investigations (Bittner and Schmeling, 1995; den Tex, 1975; Talbot, 1979; Weinberg and Schmeling, 1992; Weinberg and Podladchikov, 1995) and more recent thermal mechanical models (Burg et al., 2004; Gerbault et al., 2016; Gerya et al., 2004; Ganne et al., 2014). The originality of our study is to use (i) the structural and metamorphic record to constrain the tectonic thermal history of the Naxos dome, (ii) the size of the first order dome and its internal subdomes to provide a proxy for the characteristic scales of the gravitational instabilities, and (iii) U Pb geochronology depicting zircon dissolution and recrystallization to provide a sensitive indicator of the timescales related to these instabilities.

2. The Naxos dome in the Attic-Cycladic metamorphic complex

The Hellenides Aegean belt formed as a result of Mesozoic Cenozoic convergence between Gondwana and Eurasia (Dewey and Sengor, 1979; Dercourt et al., 1986) marked by slab retreat since at least

* Corresponding author.
E-mail address: olivier.vanderhaeghe@get.omp.eu (O. Vanderhaeghe).

https://doi.org/10.1016/j.tecto.2018.03.007

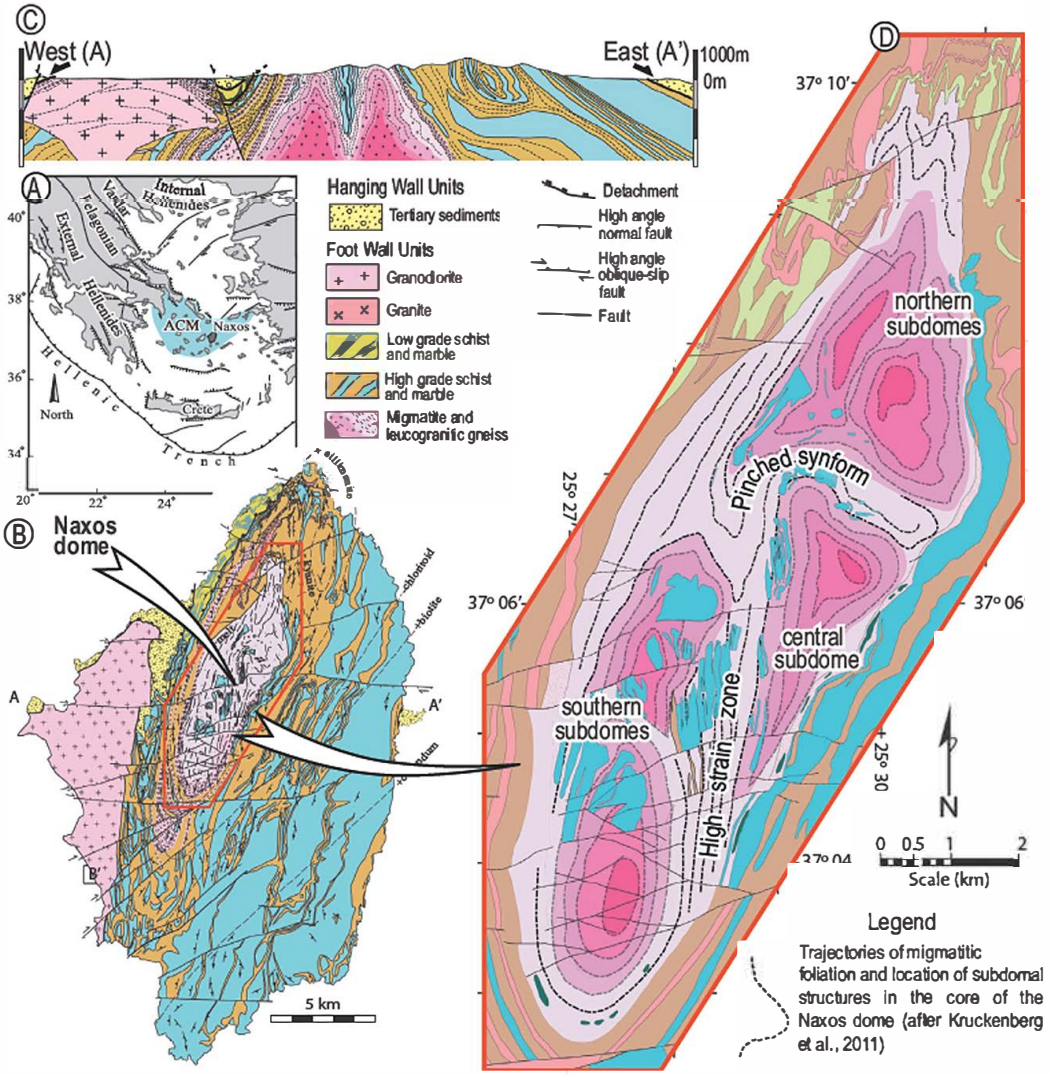

Fig. 1. Geologic map of the Naxos migmatite dome and its associated subdomes. A. Location map of Naxos Island within the Attic-Cycladic Metamorphic Complex, part of the Hellenides. B. Geological map of Naxos modified from Vanderhaeghe et al. (2007), Kruckenberg et al. (2011), and Siebenaller et al. (2013). C. East-West cross section of the Naxos dome, corresponding to the map location shown in Fig. 1B. E. Simplified geological map from Kruckenberg et al. (2011) showing subdomes delineated by synmigmatitic foliation and entrained metasedimentary septa within the migmatitic core of the Naxos dome.

Miocene times (Fytikas et al., 1984; Spakman, 1986; Wortel and Spakman, 2000). Tectonic reconstructions indicate that the orogenic crust was approximately 50 km thick, such as in the Alps, and was subsequently affected by gravitational collapse (Gautier et al., 1999; Jolivet and Brun, 2010; Ring et al., 2010; Vanderhaeghe and Teyssier, 2001) to reach the current day crustal thickness of 20–25 km (Tirel et al., 2004).

Naxos Island, in the central part of the Cyclades (Fig. 1), exposes a unique structural section into the deep orogenic root of the Aegean belt, exhumed in the core of the Attic Cycladic Metamorphic Complex (Dürr et al., 1978; Jacobshagen, 1986; Vanderhaeghe et al., 2007). It displays a dome structure cored by migmatites and mantled by a metasedimentary sequence comprised of alternating schist and marble layers (Jansen, 1973). Relics of blueschist facies metamorphism, preserved at the southern tip of the island (Avigad, 1998), have been dated at ca. 50 *Ma* by argon thermochronology (Wijbrans and McDougall, 1988) and attest for Eocene exhumation of previously subducted continental and oceanic units. These HP/LT metamorphic rocks have been overprinted by high temperature metamorphism grading from greenschist facies to amphibolite facies conditions (Buick and Holland, 1989; Duchêne et al., 2006; Jansen and Schuiling, 1976). This retrogression is attributed to post-thickening thermal relaxation of the orogenic crust associated with some exhumation (Duchêne et al., 2006). High temperature metamorphism reached partial melting conditions, as shown by the presence of migmatites in the core of the Naxos dome (Jansen and Schuiling, 1976).

Kyanite-bearing paragneisses at the contact with the migmatites record temperatures clustering around 650 °C at a pressure of 0.7–0.8 GPa (Buick and Holland, 1989; Duchêne et al., 2006), equivalent to a depth of about 27 km (considering an average density of 2.7 for crustal rocks). Given the metapelitic composition of the paragneiss, these conditions are very close to the granitic wet solidus for rocks currently just above the contact with the migmatites and are interpreted to reflect the geotherm after crustal thickening and before dome formation (Duchêne et al., 2006). Adding to these 27 km, the current day crustal thickness of 20–25 km beneath the Aegean domain leads to a minimum initial crustal thickness of 47 to 52 km thick at the climax of tectonic accretion. Migmatites within the core of the dome record a temperature of ca. 600 °C for a pressure of 0.4–0.6 GPa, corresponding to a depth of about 18 km. This pressure contrast of 0.25 GPa between the pressure peak recorded by the Ky-bearing paragneisses and by the migmatites that are now at the same exposure level has been interpreted to reflect the development of the migmatite dome after regional exhumation by ca. 9 km of unroofing (Duchêne et al., 2006).

Considering the current day thickness of 20 25 km beneath the Cyclades, we infer a thickness of about 20 km for the partially molten layer before exhumation of the migmatites to the surface.

Partial melting and crystallization of the migmatites has been bracketed to the Miocene between ca. 24 *Ma* and ca 12 *Ma* by U Pb geochronology on zircon from the migmatites and crustal derived S type granitic dikes intrusive in the mantling metasedimentary sequence, respectively (Keay et al., 2001; Martin et al., 2006, 2008). Low temperature thermochronology in the migmatites and mantling schists units indicates that they cooled from ~300 °C to ~80 °C between 12 and 9 *Ma* (Brichau et al., 2006; Seward et al., 2009). The migmatitic core and the mantling metasedimentary rocks are juxtaposed to upper crustal low grade rocks and Miocene detrital sediments along a low angle detachment (Gautier et al., 1993). The activity of the detachment is marked by the syntectonic intrusion of an I type granodiorite pluton, exposed along the western coast of the island and dated at ca. 12 *Ma* (Keay et al., 2001). The calc alkaline nature of the granodiorite and the presence of entrained mafic xenoliths point to the contribution of mantle melts in relation to lithospheric thinning and asthenospheric upwelling owing to slab retreat at this time (Altherr and Siebel, 2002; Pe Piper and Piper, 2007).

As for many migmatite domes worldwide, the tectonic significance of the Naxos dome has been debated. Jansen and Schuiling (1976) recognized the importance of partial melting and first suggested that the dome results from a diapiric rise of the migmatites. Gautier et al. (1993) refined this model proposing that the dome corresponds to upwelling of the low viscosity migmatites during regional extension accommodated by a low angle detachment. More recently, Rey et al. (2011) advocated that flow of the low viscosity migmatites into the dilatant jog resulting from localized extension was mainly isostasy driven leading to the formation of double domes. Alternatively, several authors considered that the Naxos dome results from fold interferences owing to the combined effects of *E* W shortening and regional top to the NNE shearing based on a detailed structural analysis of folds (Avigad et al., 2001; Buick, 1991). In the following section, we propose a model that builds on these studies and on a synthesis of more recently acquired structural data advocating for the predominance of gravitational instabilities in the formation of the dome and subdomes (Kruckenberg et al., 2010, 2011; Vanderhaeghe, 2004).

3. Naxos dome structure

The core of the Naxos dome is dominated by diatexites (i.e. former heterogeneous granitic magmas containing abundant metasedimentary septa of predominantly marble and schist) surrounded by metatexites (i.e. former partially molten rocks) with a dominantly paragneissic protolith (Vanderhaeghe, 2004) (Figs. 1 & 2). Structures within the migmatites of the dome preserve abundant evidence for melt present deformation that is only locally overprinted by high temperature subsolidus intracrystalline deformation (Kruckenberg et al., 2010, 2011). The contact of the migmatite dome is typically delineated by sharp transitions between granite dominated diatexite and enveloping marble units. In particular, the southern edge of the dome is delineated by a km thick zone of leucogneiss showing pervasive solid state deformation. Locally, the contact between the envelope and the core of the dome is nevertheless expressed by a diffuse contact between diatexite, metatexite and schist layers interpreted as a gradational partial melting front (Fig. 2A). Detailed structural analysis of the migmatitic core of the Naxos dome has revealed a complex pattern of migmatitic foliation and layers of metasedimentary septa dominated by marble that delineate five km scale contiguous subdomes, separated by pinched synforms and high strain zones (Kruckenberg et al., 2011) (Fig. 1). In the central and northern region of the migmatite core, the subdomes have a vertical axis of symmetry and a distributed mineral lineation of variable plunge. Trends of synmigmatitic foliation are highly variable within the subdomes, and are commonly steeply dipping to overturn resulting in a mushroom shaped three dimensional geometry (Fig. 3). The north eastern subdome is overturned along its western edge, whereas the central subdome (Fig. 1) is overturned toward the north, in accordance with the regional scale bottom south sense of shear (Kruckenberg et al., 2011; Vanderhaeghe, 2004). To the south, the subdomes are elongated and transposed along a N S trending high strain zone marked by high temperature intracrystalline deformation and a shallow dipping stretching lineation (Kruckenberg et al., 2011). The development of the Naxos dome is further recorded by transposition of granitic dikes structurally rooted in the migmatitic core (Vanderhaeghe, 2004).

These structural features are characteristic of the dome's core and are not consistent with structural trends in the mantling metasedimentary sequence, which is marked by superimposed folds with shallowly dipping axes deflected and cross cut by the migmatites coring the dome (Urai et al., 1990; Buick, 1991; Vanderhaeghe, 2004). This indicates mechanical decoupling between the mantling metasdimentary sequence and the migmatite coring the dome, thus ruling out a fold interference model (Kruckenberg et al., 2011). The subdome structures might then be interpreted as resulting either from gravitational instabilities in the low density partially molten to magmatic crust, or as isostatic driven flow of the low viscosity migmatitic layer. Isostatic driven flow should lead to the formation of double domes (Rey et al., 2011) a scenario that is not consistent with the complex subdome geometries identified by the detailed structural analysis in Naxos, nor by the multiple vertical shear zones and variably oriented pinched synforms that separate them. This structure is thus more in line with the development of adjacent diapirs or imbricated polydiapirs developing simultaneously in the core of a larger rising dome and even with the development of convection within the partially molten layer (Kruckenberg et al., 2011; Vanderhaeghe, 2004; Weinberg and Schmeling, 1992).

Nevertheless it is difficult to choose among these models from the structural analysis alone. In the following, we integrate the U Pb geochronological record of zircon grains found in migmatites and granitic dikes rooted in the dome's core, and present a first order mechanical analysis of the Naxos dome and its subdomes, in order to revisit their possible genetic significance.

4. Geochronological record of Naxos dome development

In order to constrain the timing of the development of the Naxos dome and its subdomes, we (i) further explored the U Pb geochronological record of zircon grains from diatexite of the dome's core previously published by Keay et al. (2001) and Martin et al. (2006, 2008), and (ii) obtained new U Pb geochronological dating on monazite and zircon from granitic dikes rooted in the diatexites and intrusive into the mantling metasedimentary sequence. The analytical method of the new data is indicated in Supplementary file S1.

The diatexites from the dome's core contain two distinct types of zircon grains, which have in common the presence of inherited magmatic cores yielding pre Alpine Carboniferous ages (Fig. 4 and Supplementary file S2). Some of these cores have a porous texture whereas others are pristine. Zircon grains with a porous core containing numerous inclusions of U and Th rich minerals, displaying convoluted zoning and corrosion gulfs (Fig. 4A), and having intermediate Th/U ratio (0.02 0.47), are interpreted as being formed by dissolution precipitation of the inherited zircon grains (Corfu et al., 2003; Martin et al., 2008; Tomaschek et al., 2003). These cores are locally surrounded by a finely crystallized rim characterized by oscillatory zoning (Fig. 4A). U Pb ages obtained on the porous core of these grains define a discordia line ranging from the age of the inherited cores to a younger intercept, pointing to various degrees of resetting of the U Pb isotopic system owing to a Cenozoic event (see Martin et al., 2008 for a detailed description and analysis of these data). Ages from the finely crystallized rim range from ca. 24 to 16 *Ma* and are attributed to growth of the zircon in a magma. Zircons with a pristine core are surrounded by a

Fig. 2. Representative structures of migmatites. A. Metatexitic paragneiss (right) grading into leucocratic diatexite with metatexitic enclaves (left) illustrating characteristic gradational contacts associated with the partial melting front. B. Crossed polarized light photomicrograph of a typical migmatite leucosome showing magmatic texture characterized by interlocking plagioclase, potassium feldspar, biotite and interstitial quartz. C. Crossed polarized light photomicrograph of a diatexite illustrating deformation bands in quartz indicative of weak recrystallization at high-temperature. D. Metatexite with a *syn*-migmatitic foliation defined by alternations of concordant leucosome and mesosome layers. E. Heterogeneous, granitic diatexite with metatexite enclaves. F. Heterogeneous granite typically coring the Naxos dome and its associated subdomes.

low luminescence finely crystallized rim with a convoluted texture and are associated with a euhedral external shape (Fig. 4B). These rims have characteristically low Th/U ratios (< 0.03) owing to high U contents (3000 4000 ppm) and are interpreted to have formed by high tem perature dissolution precipitation of zircon in the presence of a silicate melt and/or a magmatic fluid (Geisler et al., 2007; Hoskin and Schaltegger, 2003; Martin et al., 2008; Rubatto, 2002; Vavra et al., 1996). These rims also have ages ranging from 24 to 16 *Ma*. Never theless, as mentioned by White and Ireland (2012), some caution should be used when interpreting ages obtained on high U metamict zircons, as they might yield older apparent ages due to differential Pb and U sputtering during SIMS analysis. However, in the case of Naxos, U Pb ages are not correlated to U content (Supplementary data S2), discarding a possible analytical artefact. A detailed transect across one of these rims evidences a spectacular age gradient from 21 ± 1 *Ma* in the inner side of the rim, to 16.4 ± 0.2 *Ma* in the outer side of the rim (Fig. 4B). The mean age obtained from these rims is 18.7 ± 2.4 *Ma* (Fig. 4C). Yet, the mean squared weighted deviation is very high (MSWD ≫ 1) and individual analytical points do not all overlap within error. This indicates an excess scatter relative to the estimated analy tical error, and suggests that this dataset corresponds to significantly different ages. This is the case, in particular, for the three analytical points obtained across the finely crystallized rim with convoluted zoning shown on Fig. 4B. Accordingly, the finely crystallized rims are interpreted as representing successive dissolution precipitation of zircon around inherited cores, and potentially as growth of new zircon for rims with oscillatory zoning. Overall, four age subgroups are dis tinguished based on zircon U Pb dating of this migmatite sample from the core of the dome (Fig. 4C): 24.2 ± 0.7 Ma, 22.1 ± 0.7 Ma, 18.5 ± 0.6 Ma and 16.6 ± 0.3 Ma, defining a recurrence interval of ca. 1 to 2 *Ma* for dissolution precipitation. It should be mentioned that Keay et al. (2001) presented U Pb ages on zircon from the Naxos migmatites with similar age ranges (20.7 to 16.8 Ma) obtained on low luminescent rims truncating inherited cores or infilling dissolution embayments. This type of texture is consistent with a succession of dissolution/precipitation of zircon and is not in favor of progressive crystallization during cooling.

In order to complement geochronologic data obtained on the mig matites, two granitic dikes that are intrusive into the mantling meta sedimentary sequence have been sampled (Fig. 5 and Supplementary files S3 and S4). One granitic dike, partially transposed in the foliation of the host metasediments and marked by intracrystalline deformation, is considered to represent an early stage of granitic magma intrusion (see Vanderhaeghe, 2004, for a more detailed analysis of the

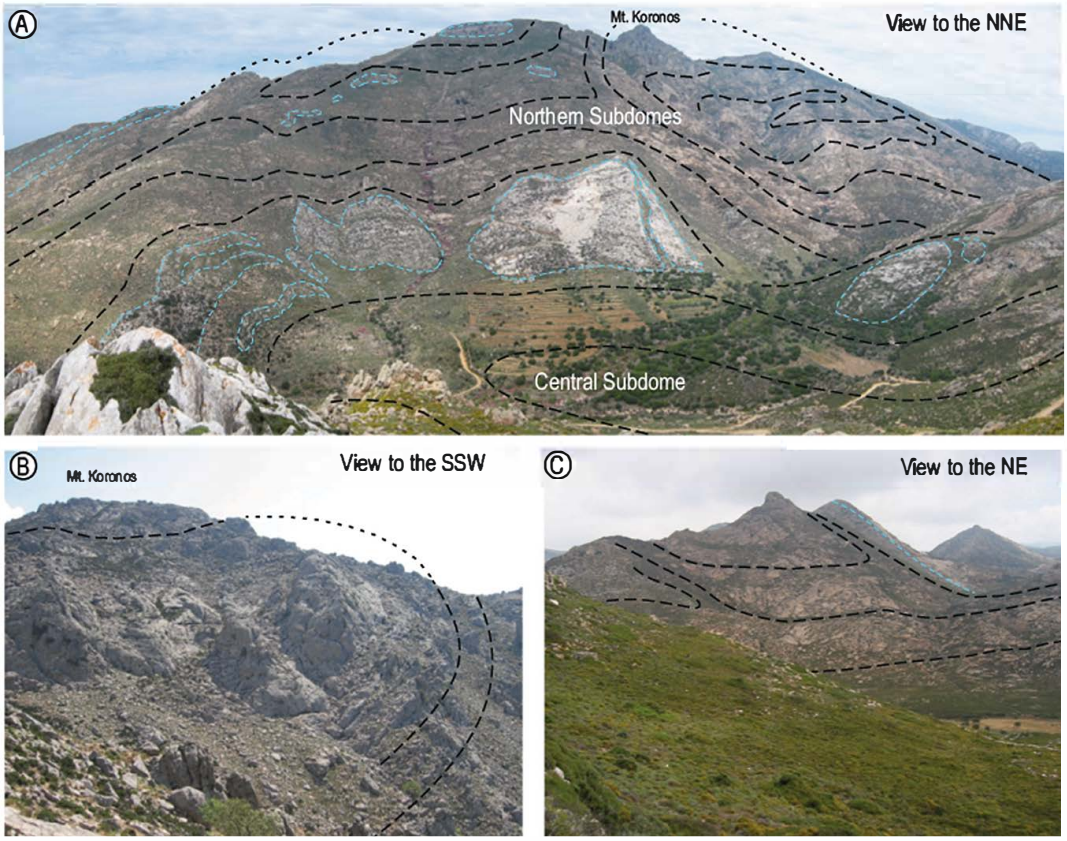

Fig. 3. Panoramic views highlighting geometric aspects of subdomes within the core of the Naxos migmatite dome. A. view to the north-northeast from near the town of Kinidharos into the migmatitic core of Naxos dome south of Mount Koronos. Here, the synmigmatitic foliation and entrained metasedimentary septa of marble delineate three subdomes: two northern subdomes, the easternmost of which is overturned on its western edge, and a central subdome whose northern edge is overturned and pinched into a tight E-W trending synform. The overturning of the marble unit is visible in this image as it transitions from vertical dipping and N-S striking in the lower left of the image, to E-W striking and S-dipping on the slope of Mount Koronos. B. View to the south-southwest of the north-facing slope of Mount Koronos showing the same overturned western side of the northern subdome shown in part A, which can be traced by a well-developed synmigmatitic foliation. C. View from within the southern subdome to the northeast of the N-S oriented synform as it trends into the N-S striking high strain zone preserved in the southern half of the dome. N.b. See Kruckenberg et al., 2011 for a detailed structural map and associated cross-sections that delineates subdomes within the core of the Naxos dome.

relationships between dome formation and dike transposition). Unfortunately the sampled dikes contain either zircon or monazite, but not both. The partially transposed dike yields a mean $^{206}Pb/^{238}U$ age on monazite of 16.1 ± 0.3 *Ma* (Fig. 5 and Supplementary data S3). The other sampled dike, displaying a magmatic fabric, being discordant to the foliation and cross cutting the partially transposed dike, represents a younger intrusive dike. This magmatic dike contains zircon crystals that yield a mean $^{206}Pb/^{238}U$ age of 13.3 ± 0.1 *Ma* confirming the relative chronology established by field relationships (Fig. 5 and Supplementary data S4). The mean squared weighted deviation (MSWD) applied to these two datasets is close to 1 indicating that individual ages do not significantly depart from the mean estimated age for each of these dikes and that the data fit a univariate normal distribution. Similar to ages obtained within the diatexites, some inherited zircon grains yield pre Alpine ages. On the other hand, two analyses obtained on zircon crystals showing cores with convoluted zones attributed to dissolution/precipitation have slightly older concordant ages of ca. 15 *Ma*. These two zircon crystals, with ages and textures equivalent to the ones of the migmatites, might represent xenocrysts entrained from the partially molten source with the segregated magma, and emplaced at a higher structural level to form the dikes.

Altogether, these data on migmatites and on granitic dikes point to a protracted U Pb geochronological record for zircon dissolution precipitation from ca. 24 to ca. 16 *Ma* in the Naxos migmatitic core, followed by successive pulses of granitic intrusions from ca. 16 to ca. 13 *Ma*. Note that Keay et al. (2001) presented U Pb ages ranging from 15.4 to 12.2 Ma on zircon from similar S type granitic dikes. This 3 to 4 *Ma* age spread obtained on syntectonic dikes provides a first order estimate to bracket the timing of dome formation, which occurred during the development and crystallization of the partially molten to magmatic core of the dome. Indeed doming could have occurred sometime before crystallization of the intrusive partially transposed dikes dated at ca. 16 *Ma*, and might have ended before the intrusion of the cross cutting dikes with a magmatic fabric dated at ca 13 *Ma*. Following this line of reasoning, we argue that the 8 *Ma* age spread of the diatexites (24 16 *Ma*) coring the dome represents the minimum time period between (i) partial melting during prograde metamorphism caused by heating of the thickened orogenic crust, and (ii) crystallization as a consequence of cooling during gravitational collapse and exhumation of the orogenic root. The duration of the presence of melt in the root of the Aegean orogenic crust might be extended to 11 *Ma* considering the bracket between the oldest zircon age in the diatexite (ca. 24 *Ma*) and the youngest age obtained on intrusive dikes (ca. 13 *Ma*).

The remaining question now is what is the significance of the age gradient from 24 to 16 *Ma* obtained on finely crystallized zircon rims? Keay et al. (2001) interpreted a similar age range (20.7 to 16.8 *Ma*), obtained on zircon grains with low luminescent rims truncating inherited cores or infilling dissolution embayments, as reflecting dissolution crystallization of zircon during partial melting. The convoluted

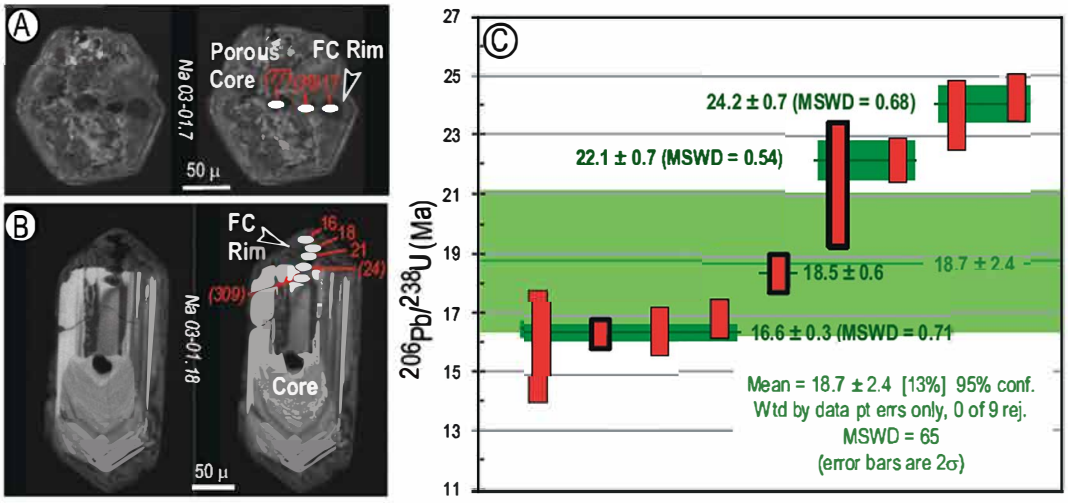

Fig. 4. U-Pb analyses of zircon from migmatite sample Na 03-01, taken within the core the Naxos dome. Numbered locations on the zircon images correspond to individual spot analyses reported in Supplementary file S2. A. Corroded zircon grain with a porous core surrounded locally by a finely crystallized rim (FC rim). U-Pb ages obtained on the porous core are partially reset and thus have no interpretable geological meaning. B. Zircon with inherited Variscan age core surrounded by a finely oscillatory zoned rim preserving an age gradient from 21 to 16 *Ma* (24 *Ma* age straddles the boundary between core and rim). C. ^{206}Pb/238U ages obtained on zircon's finely crystallized rims with error margins at 2 sigma. Ages obtained on zircon 4B are indicated with a thicker black contour. The mean age of 18.7 ± 2.4 is indicated by a dark green line with error range corresponding to the light green stripe. The MSWD is much > 1 indicating an excess scatter relative to the predicted analytical uncertainties. Four subgroups with distinct mean ages (indicated by a green dark line) are distinguished with their error range (indicated by a lighter thick green stripe). These ages are significantly different and point to pulses of zircon dissolution/precipitation of 1 to 2 *Ma*. (For interpretation of the references to colour in this figure legend, the reader is referred to the web version of this article.)

zoning of the finely crystalized rim illustrated in Fig. 4B, and the in filling of dissolution embayments described by Keay et al. (2001), are not in favor of a progressive cooling. In order to account for the distinct age peaks obtained on these grains, Keay et al. (2001) tentatively in voked the impact of discrete thermal pulses associated with repeated partial melting/crystallization cycles, locally causing the growth of new zircon. Alternatively, successive dissolution/crystallization of zircon may be due to chemical disequilibria following successive input of new zircon undersaturated magma through melt percolation (Corfu et al., 2003). Here, we explore a third possibility, that the succession of dis solution and crystallization cycles over 8 *Ma* reflects the entrainment of the zircon grains within a convecting partially molten crust, recurrently above and below zircon saturation conditions in terms of temperature and, potentially, chemistry. The difference in ages obtained on zircon rims is consistent with cycles of 1 to 2 *Ma* (Fig. 4). Note that relative to the zircon's reference frame, all of these propositions are equivalent, as they all result in varying the temperature and chemical environment of zircon grains (Fig. 6). Accordingly, U Pb geochronology on zircon on its own is not capable to discriminate between these propositions. Never theless, our preference for the convection model over the proposition of a succession of thermal pulses associated with the sporadic and loca lized circulation of fluids in the migmatites is motivated by the absence of features indicative of localized high temperature hydrothermal al teration in the rocks hosting the dated zircon grains.

5. Mechanical analysis of the Naxos dome system

In order to test the pertinence of the model invoked above, we present first order analyses of the Naxos dome system that assesses its potential to develop convective and diapiric instabilities. We evaluate (i) the viscosity of the Aegean partially molten crust required to exceed the critical Rayleigh number and enable convection, (ii) the Stokes velocity of the secondary domes (i.e. subdomes), modeled as buoyant spheres rising through a viscous matrix, and (iii) the viscosity contrast that controls the growth rate and wavelength of diapirism according to the formulation proposed by Burg et al. (2004).

The characteristic length and time scales of the system are given by the present day structure of the Naxos domes and its geochronological record. The P T conditions recorded by the metamorphic rocks, syn thesized above, indicate that the thickness of the partially molten crust (H) would have been approximately 20 km, considering that the granitic solidus was located at about 20 km depth (PT conditions of kyanite bearing paragneisses), and that the orogenic Moho attained at least 40 km depth (given the present day Moho depth of 20 25 km throughout the Aegean domain, which is located beneath rocks that exhumed from 20 km depth).

The Rayleigh number is estimated assuming two distinct thermal sources, namely basal heating and internal heating (e.g. McKenzie et al., 1974; Fig. 7). Basal heating might adequately model an increased mantle heat flux caused by thinning of the lithospheric mantle and asthenospheric upwelling in a context of slab retreat, which applies to the Aegean domain (Vanderhaeghe and Duchêne, 2010). In this case the Rayleigh number is expressed by:

$$Ra_b = \frac{\rho g \alpha \Delta T H^3}{\eta \kappa},$$

where ρ is the density, g is the gravitational acceleration, α is the thermal expansivity, ΔT is the difference in temperature between the top and the bottom of the crustal layer, H is the thickness of the crustal layer, η is the viscosity and κ is the thermal diffusivity. The condition for convection is estimated by considering typical values for these parameters for partially molten rocks (see Table 1) and assuming (i) a temperature of about 600 °C at 20 km depth at the boundary between the top of the partially molten root and the overlying solid metasedi mentary sequence, and (ii) a basal Moho temperature of 900 °C, a rather conservative choice considering a standard temperature of the asthe nosphere of 1300 °C.

The alternative thermal source results from internal heating of the orogenic crust by the decay of radioactive isotopes. In this case the Rayleigh number is expressed by:

$$Ra_i = \frac{\rho^2 g A H^5}{\eta k k}.$$

The radioactive heat production A of paragneisses and migmatites exposed on Naxos, estimated on the basis of their U, Th and K contents,

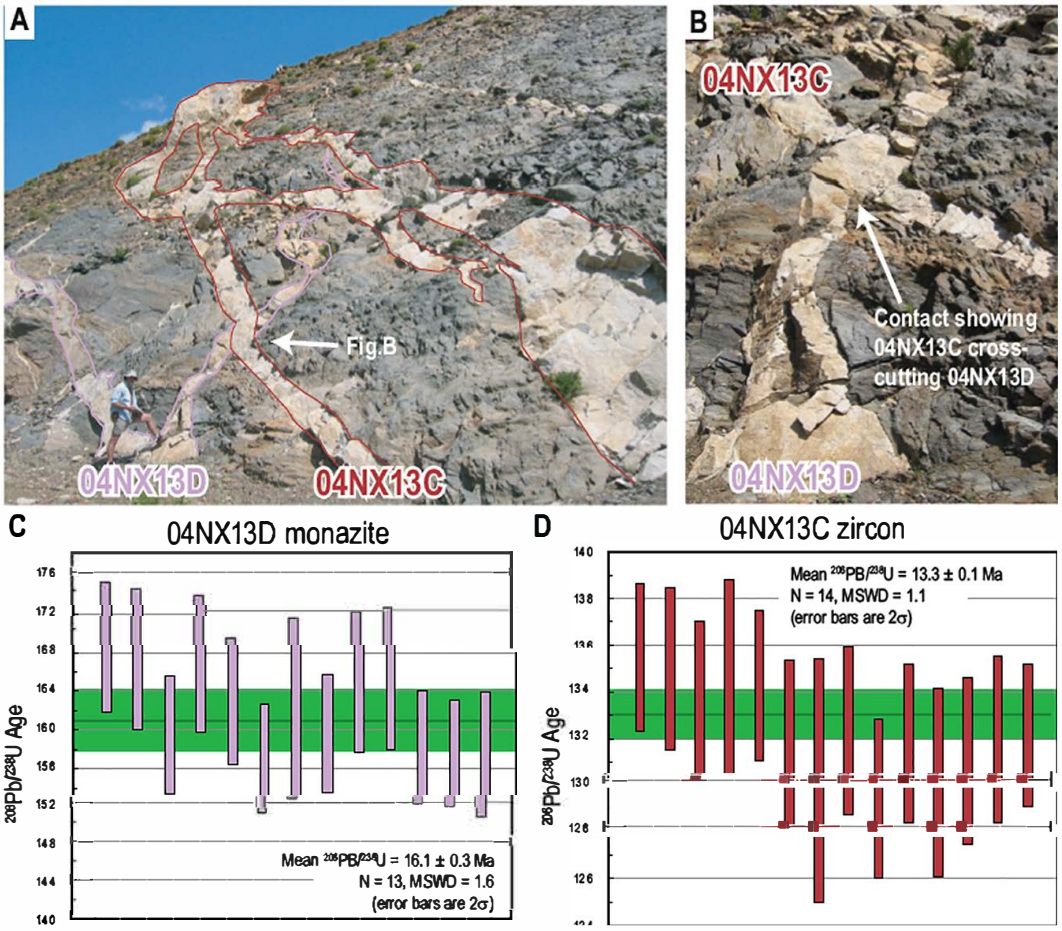

Fig. 5. U-Pb dating of transposed and discordant granitic veins. A. Field photos of the granitic dike network that is structurally rooted in the migmatites comprising the dome core. B. Close up of cross cutting dike relationships in Fig. 5A, where sampled locality 04NX13D is from a partially transposed dike that is in turn crosscut by a second generation dike (sample 04NX13C). C. U-Pb ages obtained on monazite grains from partially transposed dike 04NX13D with a mean age of 16.1 ± 0.3 Ma. D. U-Pb ages obtained on zircon grains from discordant magmatic vein 04NX13C with a mean age of 13.3 ± 0.1. Mean ages are indicated by dark green lines and error ranges by light green stripes. The MSWD applied to these datasets is close to 1 confirming the univariate distribution. The analytical method is detailed in Supplementary file S1 and additional geochronological data on these dikes are provided in Supplementary files S2 and S3. (For interpretation of the references to colour in this figure legend, the reader is referred to the web version of this article.)

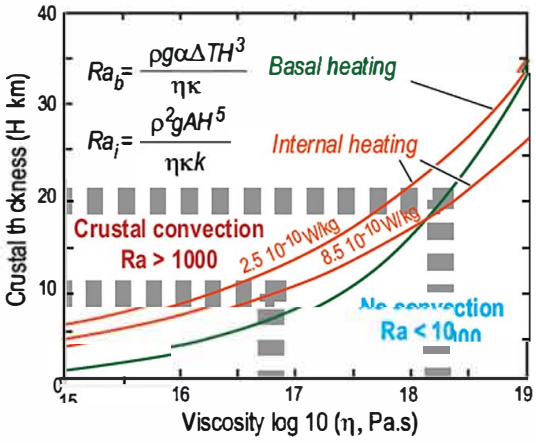

Fig. 6. Rayleigh number assessment based on the characteristics of the Naxos dome. Convection can occur if the Rayleigh number exceeds 1000, which, for a 20 km thick partially molten crust requires a viscosity of less than ca. 10^{18} Pa·s (thick grey dashed line). Rayleigh numbers are calculated for a crust heated from below or with internal heat sources (see text for details and Table 1 for parameters values).

ranges from $2.5 \cdot 10^{-10}$ W/kg to $9 \cdot 10^{-10}$ W/kg (Table 1). The thermal conductivity of granitic rocks (k) is typically 2.5 W/m/K (Mottaghy et al., 2008).

For both basal and internal heat sources, the critical Rayleigh number (~10^3, McKenzie et al., 1974) is reached if the average viscosity (η) is lower than about 2.10^{18} Pa·s for a crustal layer 20 km thick, and lower than 5.10^{17} Pa·s for a crustal layer 10 km thick (Fig. 6). Such a viscosity range stands within the spectrum of experimentally determined viscosity of partially molten rocks (see review in Rosenberg and Handy, 2005) and is higher by several orders of magnitude than the viscosity of felsic magmas (Scaillet et al., 1998; Spera et al., 1988), thereby suggesting that convection is a plausible mechanism within partially molten orogenic roots.

The relevance of this scenario of convective instability is further evaluated by calculating the velocity at which a zircon grain could revolve around an elongated convective cell of height r_1 = 10 20 km, width r_2 = 2 3 km (the typical size of the subdomes), and a revolution time of t = 1 2 *Ma*, as constrained by the estimated thickness of the partially molten crust, the typical size of the subdomes, and the recurrence period of dissolution precipitation cycles in zircon grains respectively. This yields a velocity of $V_a = 2(r1 + r2)/t$ = 1 5 cm/yr.

In parallel, we also approximate the convection cells as rising buoyant spheres in a medium of homogeneous average bulk viscosity (e.g. Weinberg and Podladchikov, 1995). Spherical bodies of

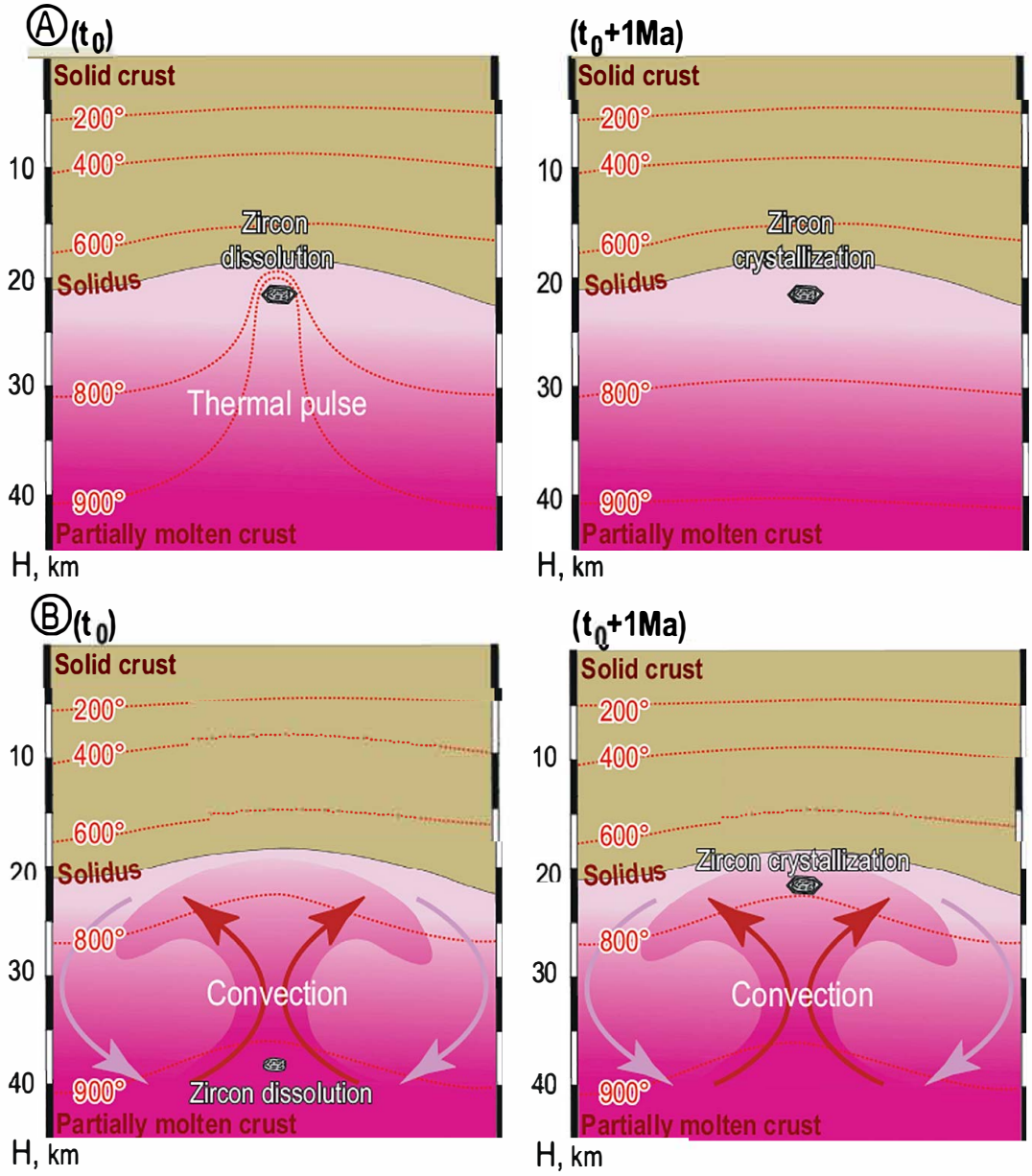

Fig. 7. Alternative models for the interpretation of U-Pb zircon ages. A. Thermal pulses affecting static zircon grains responsible for successive dissolution and precipitation. B. Convection of the partially molten layer entraining zircon grains and causing successive cycles of dissolution and precipitation.

migmatites of radius r_2 = 2 3 km with a density contrast $\delta\rho$ = 100 kg/m^3 are assumed to rise through a host matrix of constant viscosity $\eta = 10^{18}$ Pa·s. The corresponding predicted Stokes velocity $V_b = 1/3.\delta\rho.g.R^2/\eta$ = 4 cm/yr, which is consistent with the revolution velocity obtained above (V_a). Accordingly, these first order estimates indicate that convection with a revolving cycle of the order of the 1 2 million years is a viable process for the geochronologic record of zircon grains within the Naxos subdomes.

Thirdly, we follow the approach presented in Burg et al. (2004) to identify the conditions favorable to develop either a folding or a diapiric instability taking into account the strain rate, the relative thickness of the crustal layers, and their viscosity and density contrasts. Even though Burg et al.'s model assumed linear constant viscosities and a compressional tectonic regime, their theoretical results may still apply at first order to the Naxos dome. With details given in Supplementary file S5, we evaluated the parameters B and B_{det} defined in Burg et al. (2004) for a strain rate ranging between 10^{-12} and 10^{-15} s^{-1}, thicknesses of crustal layers from 5 to 20 km, viscosities between 10^{17} and 10^{20} Pa·s, and a density contrast between 100 and 200 kg/m^3. The resulting growth rate of the density driven diapiric instability is nearly in all cases > 2 orders of magnitude faster than that of the tectonically driven folding instability. However, in order to produce a dome spacing on the order of 15 km or less as observed in Naxos ($\lambda/H \sim 1$), the viscosity contrast between the buoyant lower crust and the overlying crust has to be rather close to 2, and certainly < 10 (more details in Supplementary file S5). This information, together with the other estimates presented above, point to an average viscosity of $5 \cdot 10^{17}$ to 10^{18} Pa·s for the partially molten orogenic root of Naxos. Naturally, the consideration of non linear viscosities, tensile boundary conditions and the three dimensionality of the system shall improve the evaluation of the thermomechanical properties that controlled the exhumation of the partially molten crust of Naxos, calling for a more elaborated numerical approach (*in preparation*).

Table 1
Physical parameters used to evaluate the crustal Rayleigh number.

Parameters for Rayleigh numbers		
Density ρ (kg/m^3)	2500	
Thermal expansivity α (°K ^{1})	3.10 ^{5}	
Temperature contrast (°K)	300	
Thermal diffusivity κ (m^2·s ^{1})	10 ^{6}	
Thermal conductivity k (Wm ^{1} K ^{1})	2,5	
Viscosity η (Pa.s ^{1})	10^{15}	10^{19}
Thickness of low-viscosity layer H (km)	5	25

U, Th, K contents and heat production of Naxos rocks

Rock types	Schist	Schist	Paragneiss	Paragneiss	Calcicgneiss	Metabasite	Metabasite	Metabasite	Metabasite	Granite	Migmatite
U (in ppm)	1071	2459	2989	2,7557	1,99	0,17	0,39	1,85	3,85	3,13	3,34
Th (in ppm)	3489	10,37	15,23	15,6923	10,3	0,1	1,42	5,59	13,5	2,8	12,3
K_2O (in %)	2,1	2,74	3,57	4,39	4,49	0,45	2,45	0,62	0,11	4,19	7,16
A (10 ^{10} W.kg ^{1})	2,58	5,94	7,98	8,11	5,97	0,32	1,46	3,47	7,37	5,02	8,59
A (μW m ^{3})	0,70	1,6	2,15	2,19	1,61	0,09	0,39	0,94	1,91	1,36	2,32

Radioactive heat release rates were calculated using values in W/kg of U = 9.81 10 5; Th = 2.64 10 5; K = 3.48 10 9 and a density of 2700 kg/m^3.

6. Discussion: the dynamics of the Naxos migmatite dome

The Naxos dome, in the central part of the Attic Cycladic Metamorphic Complex, is a crustal scale structure cored by migmatites and heterogeneous granites exhumed beneath an extensional crustal detachment system. While the development of the Naxos dome has been variably attributed to a number of mechanisms (e.g., diapirism: Jansen and Schuiling, 1976 and Vanderhaeghe, 2004; exhumation during regional extension: Gautier et al., 1993; Rey et al., 2011; Le Pourhiet et al., 2012; and superposed folding resulting from E W re gional shortening followed by top to the NNE shearing: Avigad et al., 2001; Buick, 1991; Urai et al., 1990) a number of structural features inherent to the migmatitic core attest to the predominance of gravita tional instabilities (cf. Kruckenberg et al., 2011): (i) *syn* migmatitic (i.e. magmatic) foliation and entrained metasedimentary septa within high melt fraction migmatites delineate numerous internal subdomes within the 5 × 12 km first order dome; (ii) structures such as synforms, cas cading folds, and triple points commonly associated with the devel opment of diapirs and convective instabilities (e.g., Ramberg, 1980) occur between subdomes, likely attesting to the downward flow of denser material in intervening regions between subdomes; and (iii) the strain pattern in the migmatite core is, in part, discontinuous with structures in mantling metasedimentary sequence (e.g., folds of the wavelength and amplitude of the subdomes and synforms do not project into equivalent structures in the enveloping units), suggesting that models invoking fold interference as the primary mechanism of dome formation are incapable of explaining the heterogeneous strain pattern and discordant structural fabrics recorded within the dome migmatites. Rather, these features are consistent with a scenario of convection of the partially molten to magmatic root of the Aegean orogenic crust, followed by diapirism and diking during orogenic gravitational collapse (Fig. 8). This model is corroborated by the quantitative assessment of the mechanical properties of the Naxos dome presented in this paper. We estimate a mean viscosity of the order of 10^{18} Pa.s or less for the partially molten to magmatic orogenic root, which, although rather conservative for partially molten felsic rocks, is conceivable when averaging the whole 10 20 km thickness of partially molten crust. The roughly axial symmetric shape of the first order dome and subdomes further attests to the key role of buoyancy driven forces in triggering gravitational instabilities in the partially molten orogenic root. Never theless, the aspect ratio (~1:2) of the first order dome indicates that regional extension of the upper crust also played a role and likely al lowed for a component of isostasy driven flow of low viscosity material (Kruckenberg et al., 2011; Rey et al., 2011).

This interpretation opens a new perspective on the interpretation of complexly zoned zircon grains with a protracted geochronological re cord typical of high grade terranes. Such zoning had been previously interpreted to be caused by repeated chemical and/or thermal mod ifications of the zircon environment causing dissolution/precipitation cycles at high temperature, in static contexts (e.g. Corfu et al., 2003; Keay et al., 2001). We propose to interpret the textural evidence of recurrent dissolution and growth of the zircon grains in the core of the Naxos dome as a chronological record of cyclic zircon entrainment in the convecting partially molten orogenic crust. Although further in vestigation of the zircon U Pb record is required to strengthen this model of the Naxos dome and the origin of its subdomes, we advocate that this interpretation is also consistent with the structural record of migmatitic deformation (Kruckenberg et al., 2011), other currently available data in Naxos, and with the first order mechanical analysis presented here.

Convection has already been proposed to account for zoning of magmatic minerals in plutons and layered intrusions (e.g. Ginibre et al., 2007) but only seldom at the crustal scale (Riel et al., 2015; Weinberg and Schmeling, 1992). According to this scenario, textural character istics and U Pb ages of zircon grains provide a proxy to estimate (i) the duration of metamorphism leading to the generation and crystallization of a melt fraction and (ii) the dynamics of convecting partially molten to magmatic layers. The duration of high temperature metamorphism associated with the presence of melt, in the case of the Naxos dome in the middle of the Aegean domain, is estimated to have lasted at least 11 Ma, when considering the difference between the oldest U Pb age obtained on a zircon grain marked by dissolution/precipitation (24 Ma) and the youngest age obtained on an intrusive granitic dike (13 Ma). An 8 Ma duration for the convective instability is bracketed by U Pb ages ranging from 24 to 16 Ma obtained on finely crystallized zircon rims within dome migmatites. The diapiric rise of the first order dome for mation is recorded by U Pb geochronology on zircon and monazite from partially transposed to cross cutting granitic veins rooting into the core of the Naxos migmatite dome, and intruding the metasedimentary mantle of the dome from ca. 16 to 13 *Ma* (~3 *Ma*). Interestingly, (i) convection of the partially molten rocks over a crustal column 10 to 20 km thick, followed by (ii) doming associated with magma extraction from the partially molten zone and intrusion in the host rocks over a relatively thinner 5 10 km crustal column could correspond to two distinct dynamic regimes that were relayed in time and accompanied the progressive thinning (collapse) of the Aegean orogenic belt.

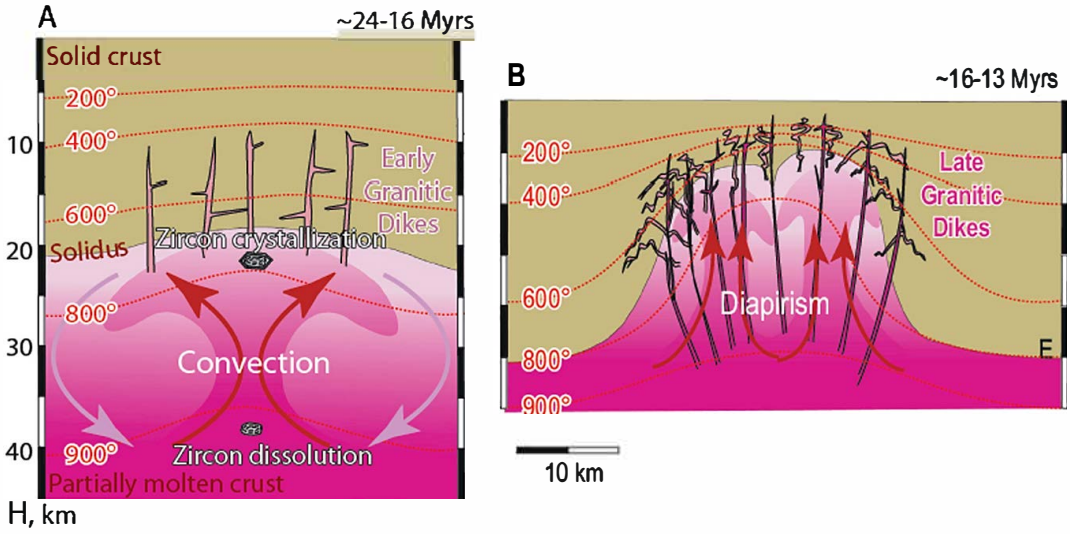

Fig. 8. Model for the internal dynamics of the Naxos dome showing the connection between crustal convection, the cyclical dissolution and crystallization of zircon, and the formation of subdomes. A. Crustal-scale convection of the partially molten orogenic root. Zircon grains are entrained with the convecting partially molten rocks and magmas. Their geochronological and textural record is interpreted to reflect dissolution at high temperature in the lower crust and crystallization at lower temperature at the top of the convective cell. The minimum duration of convection is given by the ages obtained on zircon's finely crystallized zones (24–16 *Ma*). B. Development of the Naxos first order dome by diapirism and associated crustal convection during orogenic gravitational collapse. The timing of dome formation is bracketed by U-Pb ages (16–13 Ma) obtained on granitic dikes transposed into the foliation and cross-cutting it.

7. Conclusion

The structural, metamorphic, and geochronological record of the Naxos dome and its constituent subdomes cored by migmatites are used as proxies to define the thermal tectonic history of the exhumed root of the Aegean orogenic belt and to assess its internal dynamics while it was partially molten. A thickness of ~20 km is estimated for the former partially molten crust based on the present day crustal thickness beneath the exhumed migmatites. This thickness was reached at the climax of crustal thickening (up to about 50 km) as attested by P T conditions recorded in Ky bearing paragneisses marking the contact with the migmatites coring the dome. U Pb ages from ca. 24 *Ma* to ca. 16 *Ma* and textures of zircon in the migmatites suggest successive dissolution and precipitation cycles with a period of 1 to 2 *Ma*. These cycles are probably controlled by temperature and/or chemical modification of the zircon's environment and we interpret them as the timescale of convective instabilities in a ca. 20 km thick partially molten layer. Dimensional analysis indicates that convection of a 20 km thick root requires a viscosity lower than 10^{18} Pa·s, which is consistent with the estimated viscosity of partially molten felsic rocks. Structural analysis and U Pb geochronology of deformed granitic dikes rooting in the migmatites record the subsequent development of the Naxos dome by diapirism from ca. 16 to 13 *Ma*. The size of the first order dome (5 × 12 km) requires that the unstable layer at the onset of diapirism was 5 to 10 km thick and presented a viscosity contrast with its envelope limited to about one order of magnitude.

These features, together with the structural record of deformation preserved in the dome migmatites, serve as a basis to elaborate a two stage model for the dynamic evolution of the partially molten root of the Aegean belt. After crustal thickening, thermal relaxation of the orogenic crust led to partial melting of a 20 km thick layer allowing for crustal scale convection for at least 8 *Ma* from ca. 24 to ca. 16 *Ma*. The formation of the 5 × 12 km Naxos dome occurred over approximately 3 *Ma* from ca. 16 to ca. 13 *Ma*, marking the transition from a convective instability to a diapiric instability during progressive thinning of the crust and gravitational collapse accompanied by progressive crystallization of the molten orogenic root.

Supplementary data to this article can be found online at https://doi.org/10.1016/j.tecto.2018.03.007.

Acknowledgements

We thank C. Mark Fanning (Australian National University, Canberra) for his assistance with SHRIMP U Pb age determinations, which were supported by NSF grant EAR 0409776 to C. Teyssier and D. L. Whitney (University of Minnesota), for the two granitic dike samples. This work has also been supported by a CNRS INSU Syster grant 2016 to Gerbault et al. We acknowledge Philippe Agard and Taras Gerya for their efficient editorial handling. We would like to thank Boris Kaus and Petr Jerabek for their acute reviews. This paper is dedicated to the memory of Genia Burov whose input on geodynamical modeling has been a great source of inspiration.

References

Altherr, R., Siebel, W., 2002. I-type plutonism in a continental back-arc setting: Miocene granitoids and monzonites from the central Aegean Sea, Greece. Contrib. Mineral. Petrol. 143 (4), 397–415.

Avigad, D., 1998. High-pressure metamorphism and cooling on SE Naxos (Cyclades, Greece). Eur. J. Mineral. 10, 1309–1319.

Avigad, D., Ziv, A., et al., 2001. Ductile and brittle shortening, extension-parallel folds and maintenance of crustal thickness in the central Aegean (Cyclades, Greece). Tectonics 20 (2), 277–287.

Bittner, D., Schmeling, H., 1995. Numerical modeling of melting processes and induced diapirism in the lower crust. Geophys. J. Int. 123, 59–70.

Brichau, S., Ring, U., Ketcham, R.A., Carter, A., Stoockli, D., Brunel, M., 2006. Constraining the long term evolution of slip rates for a major extensional fault system in the central Aegean, Greece, using thermochronology. Earth Planet. Sci. Lett. 241, 293–306.

Brun, J.P., Gapais, D., Le Theoff, B., 1981. The mantled gneiss domes of Kuopio (Finland): interfering diapirs. Tectonophysics 74, 283–304.

Buick, I.S., 1991. The late Alpine evolution of an extensional shear zone, Naxos, Greece. J. Geol. Soc. Lond. 148, 93–103.

Buick, I.S., Holland, T.J.B., 1989. The P-T-t path associated with crustal extension, Naxos, Cyclades, Greece. J. Geol. Soc. Lond. 43, 365–369.

Burg, J.-P., Kaus, B.J.P., Podladchikov, Y.Y., 2004. Dome structures in collision orogens: mechanical investigation of the gravity/compression interplay. In: Whitney, D.L., Teyssier, C., Siddoway, C.S. (Eds.), Gneiss Domes in Orogeny: Boulder, Colorado. Geological Society of America Special Paper 380. pp. 47–66.

Corfu, F., Hanchar, J.M., Hoskin, P.W.O., Kinny, P.D., 2003. Atlas of zircon textures. Rev. Mineral. Geochem. 53, 469–500.

Davis, G.A., Lister, G.S., 1988. Detachment faulting in continental extension: perspectives from the southwestern U.S. Cordillera: Boulder, Colorado. Geol. Soc. Am. Spec. Pap. 218, 133–159.

Den Tex, E., 1975. Thermally mantled gneissdomes; the case for convective heat flow in more or less solid orogenic basement. In: Borradaile, G.J., Ritsema, A.R., Rondeel, H.E., Simon, O.J. (Eds.), Progress in Geodynamics: Geodynamics Project, Scientific Report. Vol. 13. pp. 62–79.

Dercourt, J., Zonenshain, L.P., et al., 1986. Geological evolution of the Tethys belt from Atlantic to the Pamir since the Lias. Tectonophysics 123, 241–315.
Dewey, J.F., Sengor, A.M.C., 1979. Aegean and surrounding regions: complex multiplate and continuous tectonics in a convergent zone. Geol. Soc. Am. Bull. 90, 84–92.
Duchêne, S., Aissa, R., Vanderhaeghe, O., 2006. Pressure-temperature-time evolution of metamorphic rocks from Naxos (Cyclades, Greece): constraints from thermo-barometry and Rb/Sr dating. Geodin. Acta 19 (5), 301–321.
Dürr, S., Keller, Altherr R.J., Okrusch, M., Seidel, E., 1978. The median Aegean crystalline belt: stratigraphy, structure, metamorphism, magmatism. In: Closs, H. (Ed.), Alps, Apennines, Hellinides, Inter-union Comm. Geodyn. Sci. Rep. Vol. 38. Schweizerbart, Stuttgart, Germany, pp. 455–477.
Eskola, P.E., 1948. The problem of mantled gneiss domes. Q. J. Geol. Soc. Lond. 104, 461–476.
Fytikas, M., Innocenti, M., et al., 1984. Tertiary to Quaternary evolution of volcanism in the Aegean region. Geol. Soc. Spec. Publ. 17, 687–699.
Ganne, J., Gerbault, M., Block, S., 2014. Thermo-mechanical modeling of lower crust exhumation—constraints from the metamorphic record of the Palaeoproterozoic Eburnean orogeny, West African Craton. Precambrian Res. 243, 88–109.
Gautier, P., Brun, J.-P., Jolivet, L., 1993. Structure and kinematics of upper Cenozoic extensional detachment on Naxos and Paros (Cyclades Islands, Greece). Tectonics 12, 1180–1194.
Gautier, P., Brun, J.-P., Moriceau, R., et al., 1999. Timing, kinematics and cause of Aegean extension: a scenario based on a comparison with simple analogue experiments. Tectonophysics 315, 31–72.
Geisler, T., Schaltegger, U., Tomaschek, F., 2007. Re-equilibration of zircon in aqueous fluids and melts. Elements 3, 43–50.
Gerbault, M., Schneider, J., Reverso-Peila, A., Corsini, M., 2016. Crustal exhumation during ongoing compression in the Variscan Maures-Tanneron Massif, France-Geological and thermo-mechanical aspects. Tectonophysics. http://dx.doi.org/10.1016/j.tecto.2016.12.019.
Gerya, T.V., Perchuk, L.L., Maresch, W.V., Willner, A.P., 2004. Inherent gravitational instability of hot continental crust. Implications for doming and diapirism in granulite facies terranes. Geol. Soc. Am. Spec. Pap. 380, 97–115.
Ginibre, C., Wörner, G., Kronz, A., 2007. Crystal zoning as an archive for magma evolution. Elements 3, 261–266.
Hoskin, P.W.O., Schaltegger, U., 2003. The composition of zircon and igneous and metamorphic petrogenesis. In: Hanchar, J.M., Hoskin, P.W.O. (Eds.), Zircon. Reviews in Mineralogy and Geochemistry. Vol. 53. Mineralogical Society of America, pp. 27–62.
Jacobshagen, V., 1986. Geologie von Griechenland, Beiträge zur regionalen Geologie der. Erde, Berlin, Gebrüder Borntraeger (363 p).
Jansen, J.B.H., 1973. Geological Map of Naxos (1/50 000). National Institute of Geology and Mining Research (1 sheet).
Jansen, J.B.H., Schuiling, R.D., 1976. Metamorphism on Naxos: petrology and geothermal gradients. Am. J. Sci. 276, 1225–1253.
Jolivet, L., Brun, J.-P., 2010. Cenozoic geodynamic evolution of the Aegean. Int. J. Earth Sci. 99, 109–138.
Keay, S., Lister, G., Buick, I., 2001. The timing of partial melting, Barrovian metamorphism and granite intrusion in the Naxos metamorphic core complex, Cyclades, Aegean Sea, Greece. Tectonophysics 342, 275–312.
Kruckenberg, S.C., Ferré, E.C., Teyssier, C., Vanderhaeghe, O., Whitney, D.L., Skord, J., Seaton, N., 2010. Viscoplastic flow in migmatites deduced from fabric anisotropy: an example from Naxos dome, Greece. J. Geophys. Res. 115 (9), B09401.
Kruckenberg, S.C., Vanderhaeghe, O., Ferré, E.C., Teyssier, C., Whitney, D.L., Chapman, A., 2011. Flow of partially molten crust and the internal dynamics of a migmatite dome, Naxos, Greece. Tectonics 30, TC3001. http://dx.doi.org/10.1029/2010TC002751.
Le Pourhiet, L., Huet, B., May, D.A., Labrousse, L., Jolivet, L., 2012. Kinematic Interpretation of the 3D Shapes of Metamorphic Core Complexes.
Ledru, P., Courrioux, G., Dallain, C., Lardeaux, J.M., Montel, J.M., Vanderhaeghe, O., Vitel, G., 2001. The Velay dome (French Massif Central): melt generation and granite emplacement during orogenic evolution. Tectonophysics 342, 207–237. http://dx.doi.org/10.1016/S0040-1951(01) 00165-2.
Martin, L., Duchêne, S., Deloule, E., Vanderhaeghe, O., 2006. The isotopic composition of zircon and garnet: a record of the metamorphic history of Naxos, Greece. Special volume "Geochronology of Metamorphism, Deformation and Metallogenesis". Lithos 87, 174–192.
Martin, L., Duchêne, S., Deloule, E., Vanderhaeghe, O., 2008. Mobility of trace elements and oxygen isotopes during metamorphism: consequences on geochemical tracing. Earth Planet. Sci. Lett. 267, 161–174.
McKenzie, D.P., Roberts, J.M., Weiss, N.O., 1974. Convection in the Earth's mantle: towards a numerical simulation. J. Fluid Mech. 62 (3), 465–538.
Mottaghy, D., Vosteen, H.-D., Schellschmidt, R., 2008. Temperature dependence of the relationship of thermal diffusivity versus thermal conductivity for crystalline rocks. Int. J. Earth Sci. 97, 435–442.
Myers, J.D., Watkins, K.P., 1985. Origin of granite-greenstone patterns, Yilgarn Block, Western Australia. Geology 13, 778–780.
Pe-Piper, G., Piper, D.J.W., 2007. Neogene backarc volcanism of the Aegean: new insights into the relationship between magmatism and tectonics. Spec. Pap. Geol. Soc. Am. 418, 17–31.
Ramberg, H., 1980. Diapirism and gravity collapse in the Scandinavian Caledonides. J. Geol. Soc. 137, 261–270. http://dx.doi.org/10.1144/gsjgs.137.3.0261.
Ramsay, J.G., 1967. Folding and Fracturing of Rocks. McGraw-Hill, New York (568 p).
Rey, P., Teyssier, C., Kruckenberg, S.C., Whitney, D.L., 2011. Viscous collision in channel explains double dome in metamorphic core complexes. Geology 39, 387–390. http://dx.doi.org/10.1130/G31587.1.
Riel, N., Mercier, J., Weinberg, R., 2015. Convection in a partially molten metasedimentary crust? Insights from the El Oro complex (Ecuador). Geology 44, 31–34.
Ring, U., Glodny, J., Will, T., et al., 2010. The Hellenic subduction system: high-pressure metamorphism, exhumation, normal faulting, and large-scale extension. Annu. Rev. Earth Planet. Sci. 38, 45–76.
Rosenberg, C.L., Handy, M.R., 2005. Experimental deformation of partially melted granite revisited: implications for the continental crust. J. Metamorph. Geol. 2005 (23), 19–28.
Rubatto, D., 2002. Zircon trace element geochemistry: partitioning with garnet and the link between U–Pb ages and metamorphism. Chem. Geol. 184, 123–138.
Scaillet, B., Holtz, F., Pichavant, M., 1998. Phase equilibrium constraints on the viscosity of silicic magmas: 1. Volcanic-plutonic comparison. J. Geophys. Res. 103, 27257–27266.
Schwerdtner, W.M., 1982. Salt stocks as natural analogues of Archean gneiss diapirs. Geol. Rundsch. 71, 370–379.
Seward, D., Vanderhaeghe, O., Siebenaller, L., Thomson, S.N., Hibsch, C., et al., 2009. Cenozoic tectonic evolution of Naxos Island through a multi-faceted approach of fission-track analysis. Geol. Soc. Lond. Spec. Publ. 321, 179–196.
Siebenaller, L., Boiron, M.-C., Vanderhaeghe, O., Hibsch, C., Jessel, M., André-Mayer, A.-S., Photiades, A., 2013. Fluid record of rock exhumation across the brittle-ductile transition during formation of a metamorphic core complex (Naxos Island, Cyclades, Greece). J. Metamorph. Geol. 31, 313–338.
Spakman, W., 1986. Subduction beneath Eurasi in connection with the Mesozoic Tethys. Geol. Mijnb. 65, 145–153.
Spera, F.J., Borgia, A., Strimple, J., Feigenson, M., 1988. Rheology of melts and magmatic suspensions: 1. Design and calibration of concentric cylinder viscometer with application to rhyolitic magma. J. Geophys. Res. 93, 10273–10294.
Steck, A., Epard, J.L., Vannay, J.C., Hunziker, J., Girard, M., Morard, A., Robyr, M., 1998. Geological transect across the Tso Morari and Spiti areas: the nappe structures of the Tethys Himalaya. Eclogae Geol. Helv. 91, 103–122.
Talbot, C.J., 1979. Infrastructural migmatitic upwelling in East Greenland interpreted as thermal convective structures. Precambrian Res. 8, 77–93.
Thompson, I.B., Connolly, J.A.D., 1995. Melting the continental crust: some thermal and petrological constraints on anatexis in continental collision zones and other tectonic settings. J. Geophys. Res. 100 (15), 565–579.
Tirel, C., Gueydan, F., Tiberi, C., Brun, J.-P., 2004. Aegean crustal thickness inferred from gravity inversion. Geodynamical implications. Earth Planet. Sci. Lett. 228 (2004), 267–280.
Tomaschek, F., Kennedy, A.K., Villa, I.M., Lagos, M., Ballhaus, C., 2003. Zircons from Syros, Cyclades, Greece—recrystallization and mobilization of zircon during high-pressure metamorphism. J. Petrol. 44, 1977–2002.
Urai, J.D., Schuilling, R.D., Jansen, J.B.H., 1990. Alpine deformation on Naxos (Greece). In: Knipe, R.J., Rutter, E.H. (Eds.), Deformation Mechanisms, Rheology and Tectonics. Geological Society Special Publications No. 54pp. 509–522.
Vanderhaeghe, O., 2004. Structural development of the Naxos migmatite dome. In: Whitney, D.L., Teyssier, C., Siddoway, C.S. (Eds.), Gneiss Domes in Orogeny. Geological Society of America Special Paper Vol. 380. pp. 211–227.
Vanderhaeghe, O., 2009. Migmatites, granites and orogeny: flow modes of partially molten rocks and magmas associated with melt/solid segregation in orogenic belts. Tectonophysics 477, 119–134.
Vanderhaeghe, O., 2012. Thermal-mechanical evolution of orogenic belts at convergent plate boundaries: a reappraisal of the orogenic cycle. J. Geodyn. 56-57, 124–145.
Vanderhaeghe, O., Duchêne, S., 2010. Crustal-scale mass transfer, geotherm and topography at convergent plate boundaries. Terra Nova 22, 315–323.
Vanderhaeghe, O., Teyssier, C., 2001. Partial melting and flow of orogens. Tectonophysics 342, 451–472.
Vanderhaeghe, O., Medvedev, S., Fullsack, P., Beaumont, C., Jamieson, R.A., 2003. Evolution of orogenic wedges and continental plateaus: insights from thermal-mechanical models with subduction basal boundary conditions. Geophys. J. Int. 153, 1–25.
Vanderhaeghe, O., Hibsch, C., Siebenaller, L., Martin, L., Duchêne, S., de St Blanquat, M., Kruckenberg, S., Fotiadis, A., 2007. Penrose conference – extending a continent – Naxos field guide. In: Lister, G., Forster, M., Ring, U. (Eds.), Inside the Aegean Metamorphic Core Complexes. Journal of the Virtual Explorer, Electronic Edition (ISSN 1441-8142, Volume 27, Paper 4).
Vavra, G., Gebauer, D., Schmid, R., Compston, W., 1996. Multiple zircon growth and recrystallization during polyphase Late Carboniferous to Triassic metamorphism in granulites of the Ivrea Zone (Southern Alps): an ion microprobe (SHRIMP) study. Contrib. Mineral. Petrol. 122, 337–358.
Weinberg, R.F., Podladchikov, Y.Y., 1995. The rise of solid-state diapirs. J. Struct. Geol. 17 (8), 1183–1195.
Weinberg, R.F., Schmeling, H., 1992. Polydiapirs: multiwavelength gravity structures. J. Struct. Geol. 14 (4), 425–436.
White, L.T., Ireland, T.R., 2012. High-uranium matrix effect in zircon and its implications for SHRIMP U–Pb age determinations. Chem. Geol. 306-307, 78–91.
Whitney, D.L., Teyssier, C., Vanderhaeghe, O., 2004. Gneiss domes and crustal flow. In: Whitney, D.L., Teyssier, C., Siddoway, C.S. (Eds.), Gneiss Domes in Orogeny. Geological Society of America Special Paper Vol. 380. pp. 15–34.
Wijbrans, J.R., McDougall, I., 1988. Metamorphic evolution of the Attic Cycladic Metamorphic Belt on Naxos (Cyclades, Greece) utilizing 40Ar/39Ar age spectrum measurements. J. Metamorph. Geol. 6, 571–594.
Wortel, M.J.R., Spakman, W., 2000. Subduction and slab detachment in the Mediterranean Carpathian region. Science 290, 1910–1917.
Yin, A., 2004. Gneiss domes and gneiss dome systems. In: Whitney, D.L. (Ed.), Gneiss Domes in Orogeny. Spec. Pap. Geol. Soc. Am. Vol. 380. pp. 1–14. http://dx.doi.org/10.1130/0-8137-2380-9.1.